Effects of Electrochemical Parameters on SCC of Stainless Steels in Simulated BWR Environments

Zhanpeng Lu, Tetsuo Shoji, Kazuhiko Sakaguchi, Fanjiang Meng, Yubing Qiu

Fracture and Reliability Research Institute, Tohoku University
Aoba 6-6-01 Aramaki Aoba-ku,, Sendai 980-8579, Japan

The effects of electrochemical parameters in terms of electrochemical potential on stress corrosion cracking growth rates of austenitic stainless steels in high temperature pure water are analyzed based on obtained experimental results and reported data. The effect of decreasing electrochemical potential is more significant in non-hardened sensitized and non-hardened stainless steels than that in strain-hardened stainless steels, which is also supported by the results of Ni-base alloys and weld metals.

Keywords: Stainless steels, Stress corrosion cracking, Boiling water reactors, Electrochemical parameters.

1. Introduction

Stress corrosion cracking (SCC) has been found in boiling water reactor components fabricated from various grades of stainless steels such as 304 stainless steel (SS), low-carbon stainless steels, N-containing stainless steels, and stabilized stainless steel [1-5]. Environmental parameters such as dissolved oxygen (DO) concentration, dissolved hydrogen (DH) concentration and the resultant electrochemical potential (ECP) have been found to have a strong effect on SCC of sensitized stainless steel in high temperature pure water. Decreasing potential by using hydrogen water chemistry (HWC) and later noble metal chemical addition has been found to be effective in mitigating SCC of sensitized 304SS [6]. Recently SCC has been found in BWR components such as reactor core shroud and primary loop-recirculation piping made of low-carbon grade stainless steels. Cracking of stabilized stainless steel in a BWR plant was also reported. Investigating the effects of environmental parameters on SCC of various stainless steels would provide information for understanding the elementary cracking process and for evaluating the mitigation effect of modifying water chemistry. Experiments were designed and performed and the obtained data are compared with reported data.

Address: Fracture and Reliability Research Institute, Tohoku University,
〒 980-8579 Aoba 6-6-1, Aramaki, Aoba-ku, Sendai, Japan.
E-mail: zhanpeng@mainte.ac.jp

2. Experimental procedures

A three-directionally (3D) 10% cold-rolled 316NG SS was used for SCC growth rate tests. The solution-annealed 316NG was cold-rolled at three directions at RT. A 2.5% reduction in thickness was achieved by the first-pass rolling. The second-pass rolling was performed perpendicular to the first rolling direction on the same plane to achieve another 2.5% reduction in thickness.
The third-pass rolling to obtain a 5% reduction in thickness was performed parallel to the second rolling direction on the plane perpendicular to that used for the first and the second rolling processes. Each pass were accomplished by multiple steps to get relatively uniform deformation along the plate thickness direction. Measurements with Fischer FERITSCOPE Ferritescope indicate a low (<1%) martensite content in the cold-rolled 316NG SS. The yield strength of the 3D cold-rolled 316NG SS is 484 MPa at RT and 354 MPa at 300°C.
Contoured double cantilever beam (CDCB) specimens were used for SCC growth rate tests. The notch direction of the specimen is parallel to the final (the third) rolling direction, which is called specimen T-L orientation. The procedures for the precracking in air, in situ precracking, and SCC tests were similar to those described previously [7]. SCC tests were performed in 288°C pure water with different dissolved oxygen (DO) and dissolved hydrogen (DH) concentrations: 1) DO=2 ppm, DH~0; 2) DO<5 ppb, DH~0; 3) DO<5 ppb, DH~1.4 ppm. During the SCC tests, the electrochemical potentials (ECP) of specimens were measured against a pressure-balanced external Ag-AgCl (0.1 mol/L KCl) reference electrode. The SCC test conditions we re only changed after the preceding steady-state crack growth rate established from the time evolution of the ACPD data. The oxide films formed on sensitized 304SS and 316L SS after immersion in 2ppm DO pure water at 288°C were measured by XPS.

3. Results and Discussion

Obtained CGR data and literature CGR data for various stainless steels in simulated BWR water as functions of electrochemical potential are summarized. ECP is adjusted by controlling DO or sometimes H_2O_2 and DH contents.

3.1 The effect of ECP on sensitized 304SS

SCC growth rates vs. ECP for sensitized 304SS in 288°C pure water [1, 4, 8] are shown in Fig. 1. A parameter called mitigation factor, F_M, is used to quantify the effect of changing ECP from ECP1 to ECP2 on CGR, Eq. (1).

$$F_M(ECP1/ECP2)=CGR(ECP1)/CGR(ECP2) \quad (1)$$

Decreasing electrochemical potential has a strong effect on lowering crack growth. For example, $F_M(0.15V_{SHE}/-0.5V_{SHE})$ is several tenths and can reach about 100. CGR at ECP less than $-0.23V_{SHE}$ is significantly lower than that at high potentials of 0.15 to 0.2 V_{SHE} [1]. The threshold ECP for mitigating SCC of sensitized 304SS in simulated BWR environments has been reported. Similar ECP threshold of about -0.23 V_{SHE} for corrosion fatigue of low alloy steel in simulated BWR environments was also reported [9].
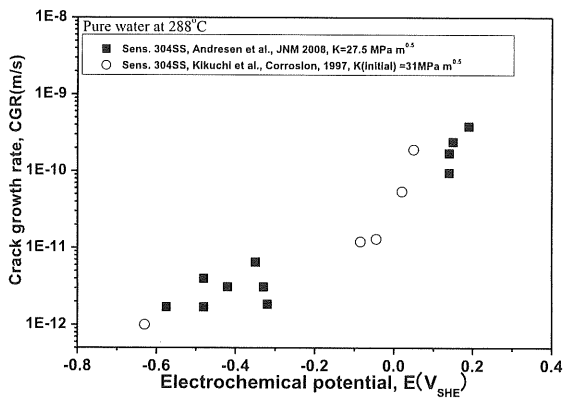

Fig. 1 Dependence of CGR on ECP for sensitized 304SS in pure water at 288°C.

3.2. The effect of ECP on non-sensitized SS

3.2.1 As-solution annealed 316L(NG) SS

SCC growth rates vs. ECP for solution-annealed low-carbon stainless steels in 288°C pure water [10] are shown in Fig. 2. Crack growth rates of SA 316L and SA 316NG SS decrease drastically with decreasing potential, which are lower than $3x10^{-12}$ m/s at ECP lower than -0.230V. At medium potential of -0.1 V_{SHE}, crack growth rates of SA low-C SS are low, close or lower than $2x10^{-12}$ m/s. The threshold ECP of about $-0.23V_{SHE}$ for mitigating SCC seems also applicable to low-C SS.
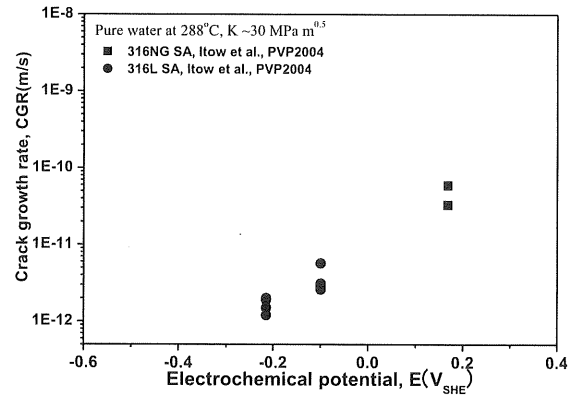

Fig. 2 Dependence of CGR on ECP for SA low-C stainless steels and 316L HAZ in pure water at 288°C [10].

3.2.2 Strain-hardened low-C SS

The ACPD results for 10% 3D CW 316NG SS (L-T orientation) under constant loading in 288°C pure water were calibrated with the measured average crack length on the fracture along the main crack path. The results at different DO and DH concentrations are shown in Fig. 3.
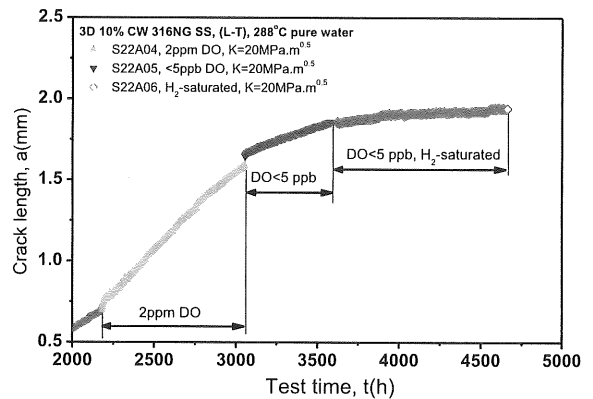

Fig. 3 Average crack length vs. test time for 10% 3D CW 316NG SS (L-T orientation) under constant loading in 288°C pure water.

Well-behaved crack growth was observed in 2ppm DO water, in deoxygenated water and in hydrogen-saturated water. CGR decreases significantly with decreasing ECP as the results of removing DO or adding DH. CGRs are calculated and plotted in Fig. 4 along with other reported data for strain-hardened low-C SS. The mitigation factor $F_M(0.2\ V_{SHE}/-0.57\ V_{SHE})$ for 3D CW316NG is about 10, which is close to the results reported by Andresen [] for 20% cool-worked 316L SS under similar applied loading level but less than that for sensitized 304SS.
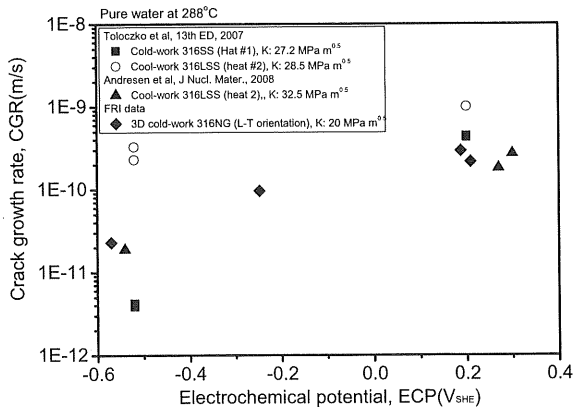
Fig. 4 Dependence of CGR on ECP for strain-hardened low-C stainless steels in pure water at 288°C [4, 11].

As shown in Fig. 4, Toloczko et al [11] has reported that the mitigation factor F_M is strongly dependent on the grain boundary properties, yield strength as the results of cold work and applied load level. F_M (2ppm DO/63ppb DH) for 20% cold worked heat #1 316SS (with 0.06 wt% C, little or no significant Mo-segregation at grain boundaries) is about 100, which is much higher than that for 21% cool-worked (at 140°C) heat #2 316L SS (with 0.014 wt% C, >10% Mo segregation at grain boundaries). FM for the later is about 3 or 4 at stress intensity factor between 25 and 30 MPa m$^{0.5}$, which becomes only 1.4 if K is in the range of 35 to 42 MPa m$^{0.5}$. The decreasing of F_M with increasing K also shows the strong mechanochemical interaction in the crack tip oxidation kinetics.

3.2.3 Ni-base alloy and weld metal

Several typical sets of CGR vs. ECP data for Ni-base alloy 600 and Alloy 182 weld metal in 288°C pure water are plotted in Fig. 5. Similar to the results of low-C stainless steel, decreasing ECP decreases CGR. F_M is high for Ni-base alloys without cold work. Cold worked Alloy 600 still exhibit a high CGR of 3.2×10^{-11} m/s at a low ECP of about -0.54 V_{SHE}.
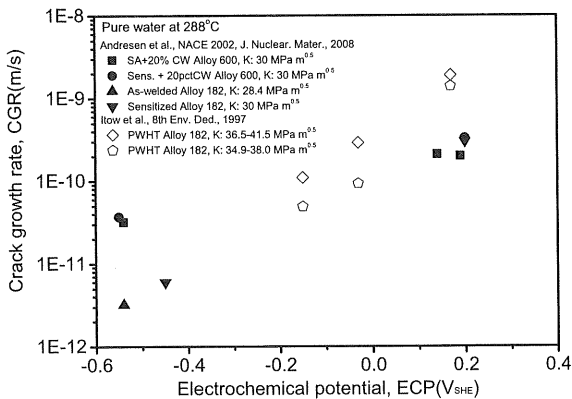

Fig. 5 Dependence of CGR on ECP for Alloy 600 and Alloy 182 in pure water at 288°C [4, 10].

3.4. Analysis of the effect of environmental parameters

Results in Figs. 1-5 imply that the effects of environmental parameters such as ECP become less significant if alloys are heavily cold worked or highly loaded. The crack growth can be viewed as a mechanochemical oxidation process. Surface oxide film plays an important role in SCC processes. The XPS results of oxide films formed on sensitized 304SS and 316L SS in 288°C pure water with 2ppm DO are shown in Figs. 6a and 6b. There is no significant difference in the values of thickness of oxide films formed on sensitized 304SS and SA 316L SS in oxygenated high temperature pure water. There is a trend that the outer oxide layer of SA 316L SS contains more nickel while has less iron. Since the data are obtained on bulk surface, more systematic analysis of local oxidation behavior especially at grain boundaries would give more insight for the environmental parameters on SCC.
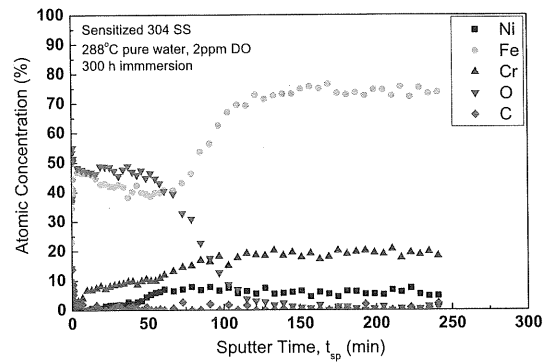
a) Sensitized 304SS
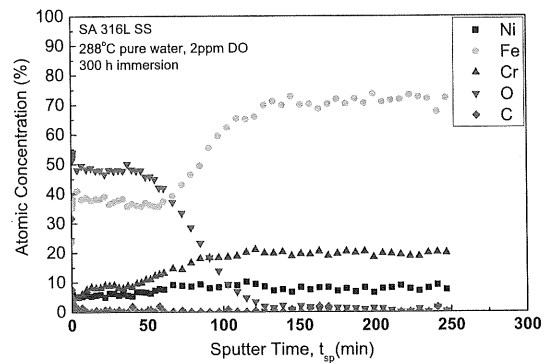
b) SA 316L SS

Fig. 6 XPS results of oxide films on a) sensitized 304SS, and b) SA 316L SS after 300h immersion 288°C pure water with 2ppm DO.

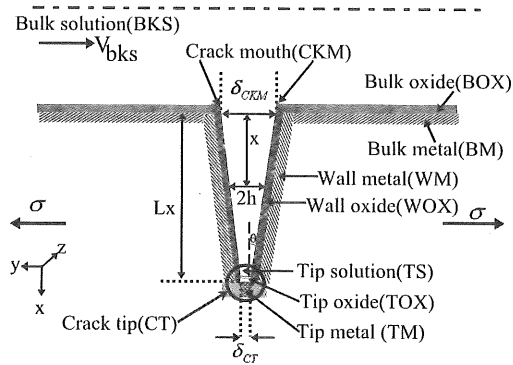The schematic of a stress corrosion cracking system is shown in Fig. 7.

Fig. 7 Schematic of a stress corrosion cracking system with different interfaces.

Crack growth rates of austenitic alloys in high temperature water can be expressed by the following equation.

$$\frac{da}{dt} = \kappa_a \cdot (\dot{\varepsilon}_{ct})^m \qquad (2)$$

Where a is the crack length, da/dt is the crack growth rate, k_a is crack tip oxidation rate constant, $\dot{\varepsilon}_{ct}$ is crack tip strain rate, m is the slope of the oxidation rate decay curve. For slip-dissolution/oxidation mechanism, there is

$$k_a = \left[\frac{M_a \cdot i_0}{z \cdot \rho \cdot F \cdot (1-m)}\right]\left(\frac{t_0}{\varepsilon_f}\right)^m \qquad (3)$$

For solid state oxidation mechanism, there is

$$k_a = [(k_1)^{(1-m)} \cdot (\varepsilon_d)^{(-m)}] \qquad (4)$$

Results in Figs. 1-5 indicate that the effect of ECP on oxidation rate constant k_a is also related to the material property such as the degree of cold work. According to slip-dissolution/oxidation mechanism, m is also function of ECP. In solid-state oxidation mechanism, it is expected that ECP would affect more the absolute value of oxidation rate than the oxidation rate law, i.e., ECP would have more significant effect on k1 than on m. Oxidation rate constant k. Oxidation kinetics at the SCC tip can be viewed as a quasi-solid state oxidation kinetics where the mass transport in the solid oxide film, the mass transport inside the crack enclave and surface electrochemistry would play important roles in determining the reaction rate. A. Turnbull [12] proposed the general equation for the mass transport in a SCC crack, Eq. (5).

$$\frac{\partial C_i}{\partial t} = D_i \frac{\partial^2 C_i}{\partial x^2} + \frac{z_i D_i F}{RT} \frac{\partial}{\partial x}(C_i \frac{\partial \varphi}{\partial x}) + \sum_j R_{i,j,homo} + \sum_j \frac{R_{i,j,hetero}}{\delta_x}$$
(5)

Where $R_{i,j,hom}$ is homogeneous equilibrium reaction process that can occur in the solution in the crack, $R_{i,j,het}$ are heterogeneous reactions processes that can occur on the walls of the crack (including redox reactions and interfacial precipitation reactions), δ_x is a half of the crack width at a distance x from the crack mouth. The interaction between crack tip mechanics and crack tip oxidation kinetics is also revealed by the different responses of CGR of cold-worked and non-cold worked

stainless steels to changing ECP by adjust DO or DH concentrations.

4. Conclusions

The effects of electrochemical potential on SCC growth rates of various austenitic SS are analyzed based on obtained experimental results and reported data. The effects of electrochemical conditions would become less significant if alloys are heavily cold-worked. The results provide crucial information for understanding mechanochemical interactions involved in SCC of materials in high temperature water and for selecting mitigation methods.

References
[1] P.L. Andresen, F.P. Ford, Mater. Sci. Eng. A 103 (1988) 167.
[2] S. Suzuki, K. Kumagayi, C. Shitara, et al., Maintenology 3 (2004) 65.
[3] T. Shoji, Proc. 11th Int. Symp. Environ. Degradation of Materials in Nuclear Power Systems–Water Reactors, held August 10–14, 2003, Skamania, Stevenson, Washington, ANS, 2003, pp. 588–598.
[4] P.L. Andresen, M.M. Morra, J. Nucl. Mater. 383 (2008) 97–111.
[5] U. Ehrnsten, H. Hanninen, P. Aaltonen, et al., Proc. 10th Int. Symp. Environmental Degradation of Materials in Nuclear Power Systems–Water Reactors, 2001, NACE, CDROM.
[6] Y.J. Kim and P.L. Andresen, Corrosion 59 (2003) 511.
[7] Z.P. Lu, T. Shoji, Y. Takeda, et al., Corros. Sci. 50 (2008) 698.
[8] E. Kikuchi, M. Itow, J. Kuniya, H. Sakamoto, M. Yamamoto, A. Sudo, S. Suzuki and M. Kitamura, Corrosion 53 (1997) 306-311.
[9] J. Congleton, T. Shoji, R.N. Parkins. Cor. Sci., 25(1985) 633.
[10] M. Itow, M. Kikuchi, N. Tanaka, et al., Proc. 2004 ASME Pressure Vessels and Piping Division Conference, ASME, 2004, pp. 167-173.
[11] M. Toloczko, M., S.M. Bruemmer, P.L. Andresen, Proc. 13th Int. Symp. Environmental Degradation of Materials in Nuclear Power Systems–Water Reactors, 2007.
[12] A. Turnbull. Corrros. Sci., 39(1997)789.